Stack, seal, evacuate, draw: A method for drawing hollow-core fiber stacks under positive and negative pressure

LEAH R. MURPHY[1,*], STEPHANOS YEROLATSITIS[1,2], TIM A. BIRKS[1], AND JAMES M. STONE[1]

[1]*Centre for Photonics and Photonic Materials, Department of Physics, University of Bath, Bath, BA2 7AY, UK*
[2]*Now at CREOL, The College of Optics and Photonics, the University of Central Florida, Orlando, Florida 32816, USA*
**lm691@bath.ac.uk*

Abstract: The two-stage stack and draw technique is an established method for fabricating microstructured fibers, including hollow-core fibers. A stack of glass elements of around a meter in length and centimeters in outer diameter forms the first stage preform, which is drawn into millimeter scale canes. The second stage preform is one of the canes, which is drawn, under active pressure, into microscopic fiber. Separately controlled pressure lines are connected to different holes or sets of holes in the cane to control the microstructure of the fiber being drawn, often relying on glues or other sealants to isolate the differently-pressured regions. We show that the selective fusion and collapse of the elements of the stack, before it is drawn to cane or fiber, allows the stack to be drawn directly under differential pressure without introducing a sealant. Three applications illustrate the advantages of this approach. First, we draw antiresonant hollow-core fiber directly from the stack without making a cane, allowing a significantly longer length of fiber to be drawn. Second, we fabricate canes under pressure, such that they are structurally more similar to the final fiber. Finally, we use the method to fabricate new types of microstructured resonators with a non-circular cross-section.

1. Introduction

1.1 Hollow-core fibers

Hollow-core fibers (HCFs) guide light in air, rather than in glass. This means that HCFs have low latency, a low nonlinear coefficient, and a high damage threshold. It also means that they can guide light at wavelengths where solid materials have high attenuation due to Rayleigh scattering, IR absorption, or photodarkening. For these reasons, HCFs have been intensely researched over the past few decades with widespread applications including high power and ultrafast pulse guidance [1,2], mid-IR [3,4] and deep-UV guidance [5–7], light-matter interactions [8], and telecommunications [9,10].

Antiresonant fibers (ARFs) are HCFs that have a microstructure consisting of a hollow core surrounded by a cladding formed of thin webs of material, usually fused silica, that provide an anti-resonant reflection condition to the light being guided in the hollow core. At wavelengths where the webs in the cladding are of antiresonant thickness relative to light in the core, light incident on the cladding reflects back into the core and so can be guided with low loss along the fiber [11]. However, the optical performance of ARFs is affected by the nodes which form where the webs intersect. Nodes are avoided in nodeless ARFs, where the cladding structure is formed of non-touching, thin-walled capillary tubes that act as resonators. The avoidance of cladding nodes reduces the confinement loss of a nodeless ARF compared to an equivalent ARF with nodes [12].

Designing and fabricating nodeless ARFs has therefore recently been the focus of significant interest, particularly for telecommunications. Over the past five years, the attenuation of nodeless ARFs has been reduced from 8 dB/km at 700 nm [13] to values relevant for data communication by modifying the structure of the resonators [14–17]. The double nested nodeless ARF currently holds the record for the lowest loss ARF with a reported attenuation of 0.174 dB/km between 1500 and 1550 nm [18].

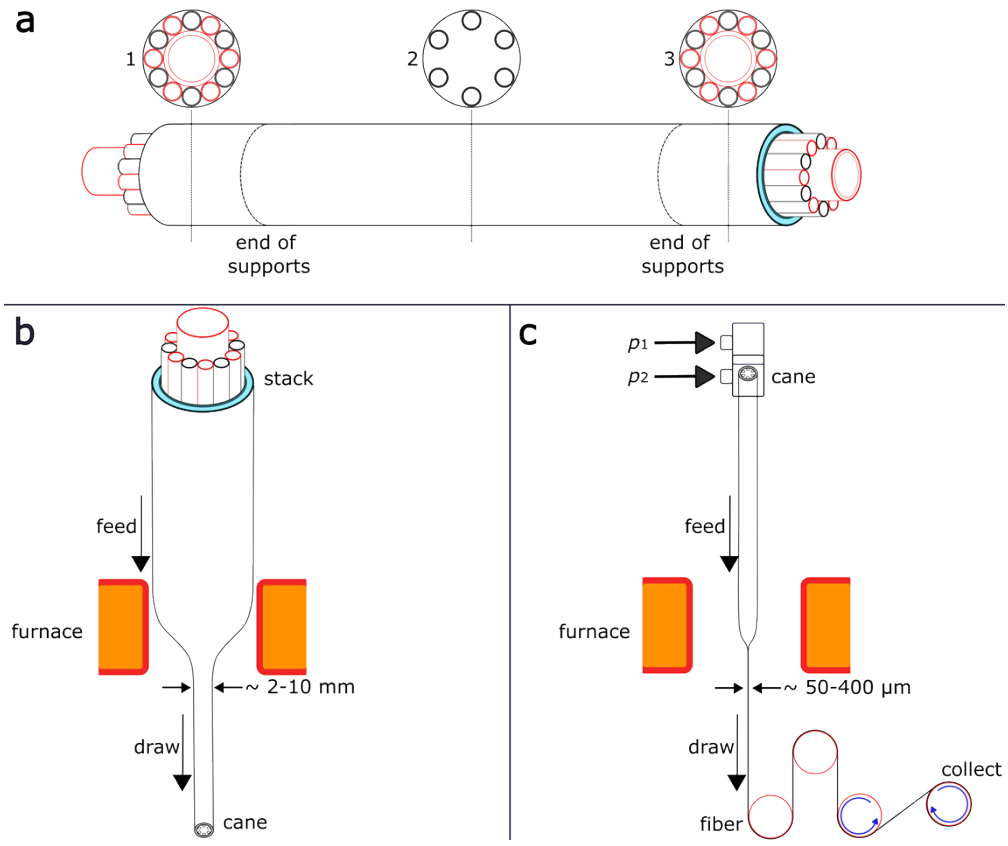

Fig. 1. Schematic diagrams of the two-stage stack and draw process for ARF fabrication. (a) A stack for a nodeless ARF with six resonator tubes. The resonators (black) extend the entire way along the stack. At each end of the stack, one support tube (red) is placed between each pair of adjacent resonator tubes, and a bigger one is placed in the center of the assembly. The supports do not extend along the entire stack but terminate a few centimeters from the ends. Cross-sections (1) and (3) show the support regions where resonators and supports are both present, while (2) shows the middle of the stack which contains the resonators only. (b) Stage 1: drawing a stack into canes on the drawing tower. (c) Stage 2: drawing a cane under pressure into nodeless ARF. The cane is generally prepared for pressurization using sealant, which is applied to the top of the cane such that the core space (pressure p_1) is isolated from the holes in the middle of the resonators (pressure p_2).

1.2 The stack and draw process

The stack-and-draw process [19] is the principal method used worldwide to fabricate ARFs [14–16, 20–22]. The preform is constructed from tubes or rods, which are typically of the order of a meter in length and millimeters in outer diameter, stacked into a larger, meter-long jacket tube with an outer diameter of a few centimeters. This structure is known as a stack. The tubes or rods are assembled such that the macroscopic structure of the stack can be drawn into the microscopic structure of the fiber under the correct conditions. A nodeless ARF stack with 6 resonator tubes is shown schematically in Fig. 1(a). The resonators need to be held in contact with the inner surface of an outer jacket tube such that they remain spaced apart and encircling the space in the middle, which will become the hollow core. One way to ensure this is to

separate the resonators with support tubes at each end that only extend a small way into the stack. Generally, one support tube is placed between each adjacent resonator, and a larger one is placed centrally in the core. Alternatively, the resonator tubes can be held in place in the stack by applying external heat to bond them to the inner surface of the outer jacket [21,24]. Once assembled, the stack can be drawn down in size through a furnace in the usual way, with a final outer diameter determined by the speeds at which the glass is fed into and drawn out of the furnace.

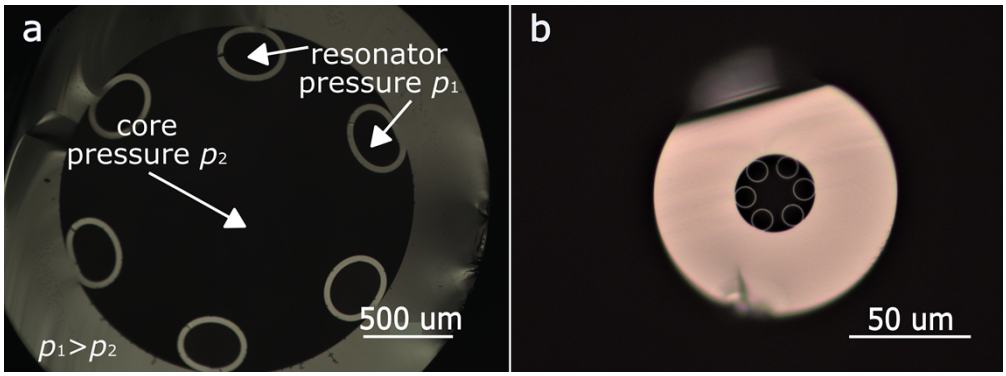

Fig. 2. (a) An optical micrograph of the cross-section of a nodeless antiresonant hollow-core cane, showing the different regions that are pressurized during the fiber draw. (b) An optical micrograph of the cross-section of a 6-resonator nodeless ARF drawn from a similar cane.

In practice, the stack-and-draw process for HCFs is usually carried out in two stages [14–16, 19–21]. First the stack is used as the preform and is drawn to glass canes [19], Fig. 1(b), with an outer diameter of around a few millimeters and a length of about a meter. The second-stage preform is one of these canes which is drawn into fiber, Fig. 1(c), with an outer diameter from tens to hundreds of micrometers. The cane may be inserted into another jacket tube before being drawn to fiber. This can help achieve a more manageable fiber outer diameter, particularly for HCFs guiding shorter-wavelength light because the core diameter and cladding wall thickness a HCF scale with wavelength. Fine control of the fiber microstructure at the second stage is important. For HCFs specifically, pressurized gas is applied independently to different air regions of the internal cane geometry during the fiber draw. This acts against the collapse of the fiber's delicate glass microstructure induced by surface tension (which makes holes shrink or collapse completely if unchecked [23]) and can be used to inflate certain air regions of the microstructure relative to others. Often, a sealant such as a UV curable adhesive or a two-part epoxy is applied to the top of the cane to block different air regions of the cane geometry from one another so that a pressure differential can be established between them. As an example, the internal structure of a nodeless ARF cane, showing the regions where different pressures p_1 and p_2 are applied, is shown in Fig. 2(a) and the cross-section of the resultant fiber is shown in Fig. 2(b).

However, a cane is much smaller than a stack, so using an intermediate cane stage limits the length of fiber that can be collected in a single draw. This is especially restrictive when fabricating ARFs with large outer diameters intended for mid-IR or multimode guidance. It is possible to get around this problem by making bigger stacks and canes, but the maximum outer diameter is practically restricted by the inner diameter of the furnace. Furthermore, Jasion *et al.* have shown using a virtual draw model that the ultimate limit on the draw down ratio is related to the fluid dynamics of the fiber draw [20]. Alternatively, the stack could be drawn directly to fiber, bypassing the cane stage altogether. For example, if a 25 mm diameter stack is drawn directly to 300 μm diameter fiber, the draw yield is 694 m per 10 cm of preform, whereas if the stack is drawn via a 7 mm diameter cane, the draw yield is 54 m per 10 cm of preform. In practice, the furnace temperature and applied pressures need to be optimized to

achieve the desired fiber microstructure before fiber can be collected, using up a portion of the length of preform. This portion can be significant if the draw down ratio between the preform and fiber is smaller and must be considered as well as the draw yield.

The use of sealants (for example, glues) during pressurization is also problematic. Sealant at the top of a preform gets hot, and then degrades, as the preform is fed into the furnace. This can cause the seal to fail, losing the required pressure differential in the preform. It can also release organic contaminants from the sealant into the preform. Such contaminants can promote devitrification in the preform as it is drawn through the furnace, weakening the fiber, and can also create scattering centers that compromise the fiber's optical performance. These problems are made worse if attempting to draw with pressurization directly from the stack. Larger volumes of sealant are needed, which increases the risk of contamination. Additionally, larger preforms don't dissipate heat as well as smaller ones, so the sealant would have to withstand higher temperatures without degrading. We consider that it is for this reason that (to our knowledge) there are no reports of an ARF stack being drawn while subject to applied pressure, to make a fiber either directly or via a cane with a structure that benefited from pressure control.

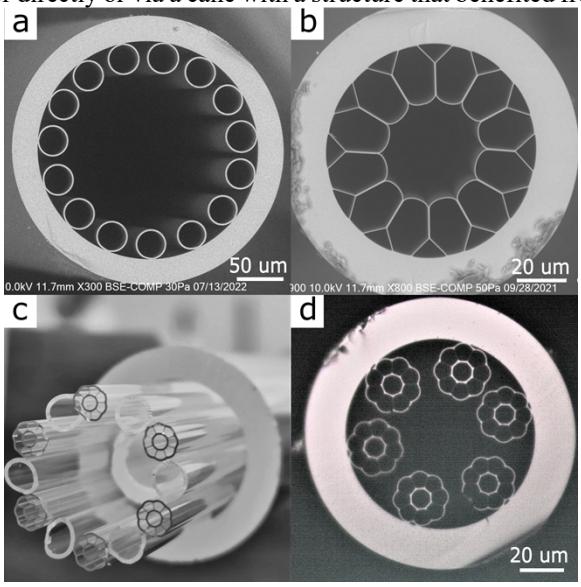

Fig. 3. Fibers that we fabricated using SSED to showcase three applications of the method. (a) An SEM of a 15-resonator ARF, drawn directly from stack, (b) an SEM of an ARF that was drawn from an almost identical cane, (c) a photograph of a stack containing "resonator-canes". The outer diameter of the stack is 25 mm, (d) an optical microscope image of the microstructured ARF drawn (via a cane stage) from the stack in (c).

In this paper we report a supplement to the stack and draw technique which we call the Stack, Seal, Evacuate, and Draw (SSED) method. By the controlled fusion of glass elements at the ends of the stack before it is drawn to cane or fiber, SSED allows different regions of the stack to be pressurized without any sealant. By presenting examples of fibers that we have fabricated using SSED (Fig. 3.), we demonstrate our method in three ways. First, by drawing the fiber shown in Fig. 3(a), we show that SSED can be used to draw an ARF from stack directly to fiber without the use of a sealant; second, by drawing the fiber shown in Fig. 3(b), we show that SSED can be used to make canes under pressure such that they are structurally similar to the fiber that they will be drawn into; finally, by fabricating the stack and fiber shown in Fig. 3(c-d), we show that SSED can be used to create new types of microstructured resonators ("resonator-canes" to be incorporated into a new stack) that require positive and/or negative pressure for their formation.

2. Stack, seal, evacuate and draw

2.1 The method

To demonstrate how to implement SSED, we drew a nodeless ARF with an outer diameter of 300 µm with a draw yield of 694 m per 10 cm of preform.

First, we stacked resonator and support elements into a meter long jacket tube. Prior to stacking, a small slit was cut 32 cm from one end of the jacket tube using a diamond saw. The resonator and support elements were then stacked inside the jacket tube in the usual way. An example stack is shown in Fig. 4(b). The purpose of the slit is to enable pressure to be applied to the interstitial air region inside the stack that surrounds the resonators and supports and includes the space that will become the fiber's core. For clarity, we will refer to the end of the stack closest to the slit as the *working end*, and the end furthest from the slit as the *closed end*.

The supports at the working end of the stack were tubes sealed at the end inside the jacket tube prior to stacking, Fig. 4(a). This is because a negative pressure will be applied through the slit whilst the working end of stack is in the furnace. The tubular supports are required to keep the other stacking elements in position, so they need to be isolated from the negative pressure inside the jacket tube. Our support tubes were sealed by applying heat to one end using a hydrogen-oxygen torch, the central holes closing under surface tension. With proper management, solid rods can be used as the supports at the working end instead of sealed tubes, but rods are heavier and generate significantly more heat when the stack is in the furnace. The outer circumference of each end of the stack is heated using a hydrogen-oxygen torch to gently fuse the stack elements to the outer jacket and prevent them from slipping out under gravity.

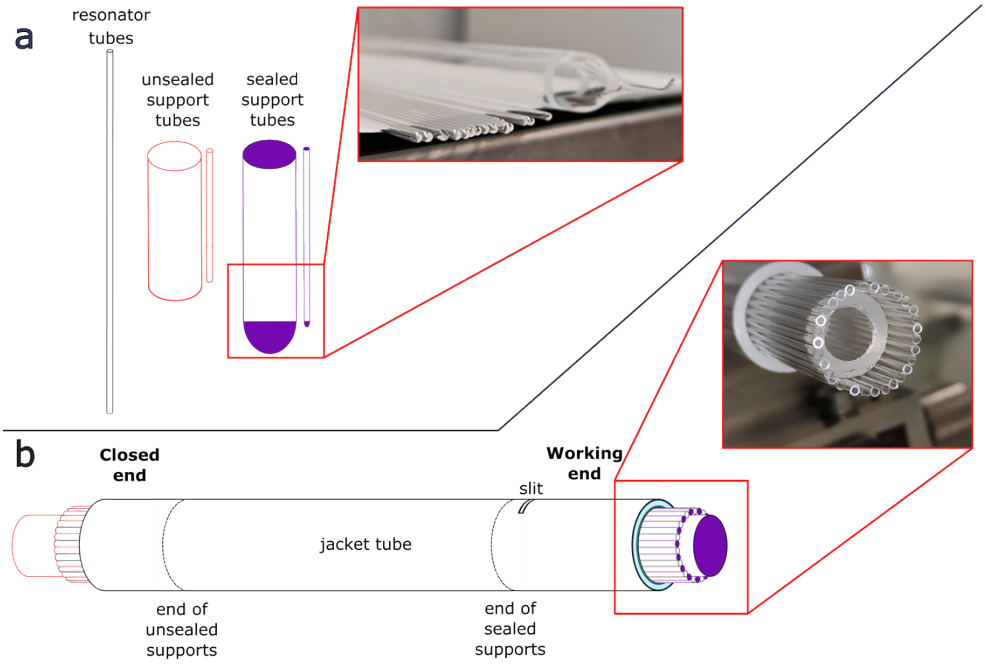

Fig. 4. Schematic diagrams of the stacking elements (a) used to construct a nodeless ARF stack (b) that has been prepared for processing by SSED to fabricate a large, 15-resonator ARF without using a cane stage. The supports at the working end (indicated with purple shading) are tubes that were sealed at one end before they were stacked with the sealed end oriented into the stack. The inset photograph in (a) shows the sealed ends of the supports. The inset photograph in (b) shows the working end-face of the stack.

Next, we fed the stack into the furnace with the closed end at the bottom and started drawing the closed end into canes. No pressure was applied at this step. We periodically inspected the cross-section of the canes under an optical microscope. When the cross-section had become symmetrical, we sealed the closed end by continuing to draw down whilst simultaneously withdrawing the stack upwards from the furnace. The closed end of the stack now comprises a symmetrically-formed neck-down region, ending in a seal. Schematic diagrams of this step are shown in Fig. 5.

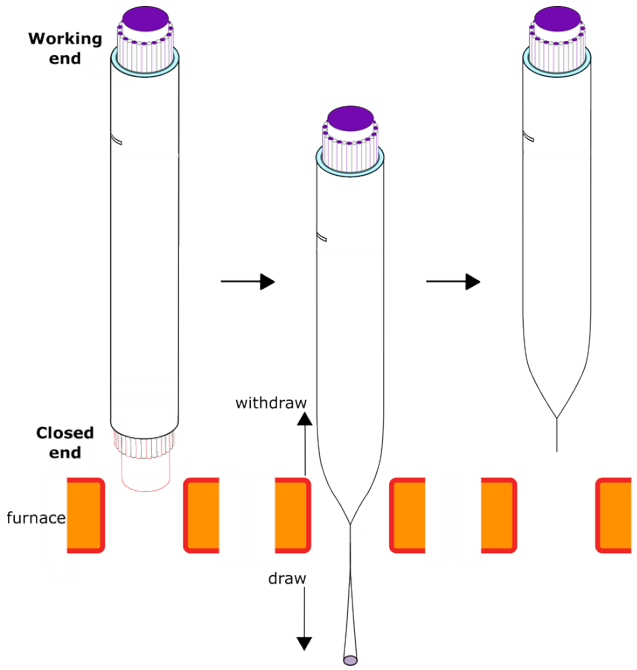

Fig. 5 Sealing the closed end of the stack by drawing it into canes whilst simultaneously withdrawing the stack upwards.

After sealing the closed end, the stack was flipped so that the closed end was at the top. We fed the working end into the furnace and started drawing it into canes while a negative pressure was applied through the slit to partially evacuate the interior of the stack. As the interior ends of any tubular supports were sealed prior to stacking and the ends of the resonator tubes protrude outside the jacket, the only part of the stack affected by the negative pressure was the interstitial air region surrounding the elements of the stack. The negative pressure therefore closed up the interstitial air region as the working end was drawn into canes, while leaving the resonator tubes and supports open. Once this was achieved (as verified by inspecting the drawn canes under the microscope) the stack was again withdrawn upwards from the furnace. Fig. 6(a) is a schematic diagram of this step, including a cross-sectional micrograph of the working end after processing. Fig. 6(b) shows how the cross-section of the working end is modified.

Finally, to draw a fiber or a cane from the stack, the stack was flipped again so that the working end was at the top and the closed end at the bottom, and the working end was cleaved such that it had a flat end face. The glass at the working end had been fused so that there was only access to the resonator tubes (the support tubes being blind holes), and the slit on the side of the jacket tube allowed access only to the interstitial air region, which includes the eventual fiber core. The result was a preform where the core space and the resonator holes were blocked from one another. Hence, the core space and resonators could be selectively pressurized, through the slit and through the working end respectively, but without the use of sealants.

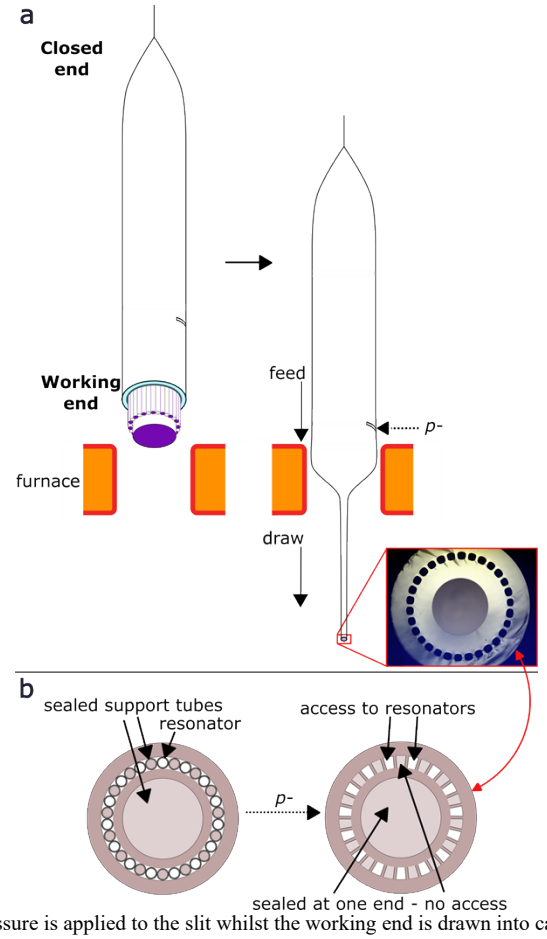

Fig. 6. (a) A negative pressure is applied to the slit whilst the working end is drawn into canes. The slit only provides access to the interstitial air region in the stack, so this alone closes where the glass is heated by the furnace. The inset is a micrograph of the prepared working end, showing the new cross-sectional structure after the end-face has been cleaved. The outer diameter of the end-face is 2.5 mm. (b) Schematic cross-sections of the working end before and after closing the interstitial air region, where the supports are tubes with their interior ends sealed. The holes visible at the working end in (a) alternate between (open) resonators and (sealed) supports.

3. Applications of SSED

3.1 Drawing an SSED stack direct to fiber

The first example application of SSED is to draw the stack described in the previous section directly to fiber, while applying a positive pressure to the resonators through the working end. A different positive pressure can also be applied the interstitial air region (including the core) through the slit cut into the jacket, Fig. 7(a). Pressure is applied to the preform via brass fittings that are attached to it using either PTFE thread seal tape or rubber O-rings. Most but not all (approximately 60%) of the preform could be drawn to fiber because the slit, and therefore any part of the stack above it, cannot be drawn through the furnace.

To show the value of this application of SSED, we drew 1 km of fiber using 24% of the usable 60% of the stack. 470 m was drawn whilst adjusting the pressures and other draw parameters to optimize the structure of the fiber, and the remaining 530 m of fiber was uniform optimized fiber. The fiber, Fig. 7(b), was designed to guide light with a wavelength of 3 μm between the first and second resonances and was fabricated to be multimode, using the principles outlined in [25]. Table 1 compares the fiber geometry of one end of the 530 m to the other, showing that the fiber microstructure remained stable throughout the draw.

Table 1. Comparing the geometry of each end of the 530 m length of fiber.

	Start of fiber			End of fiber		
	Minimum	Maximum	Average	Minimum	Maximum	Average
Core diameter / µm	172 ± 1	177 ± 1	174 ± 3	170 ± 1	176.3 ± 0.8	174 ± 4
Resonator diameter / µm	32.1 ± 0.3	35.0 ± 0.2	34 ± 1	31.3 ± 0.4	34.5 ± 0.2	33.2 ± 0.8
Resonator thickness / µm	2.00 ± 0.02	2.35 ± 0.06	2.20 ± 0.18	2.16 ± 0.13	2.45 ± 0.05	2.25 ± 0.21

We did not have time to draw more than 1 km of fiber in our fabrication session, but a continuous 4.1 km length of the fiber could have been drawn from the SSED preform, including the portion that is drawn in the process of optimizing the structure of the fiber. If the stack had first been drawn to a cane with the representative diameter of 7 mm and representative length of 1 m, the total continuous length of fiber that could be drawn is 490 m (assuming 90% of the length of the cane were drawn into fiber).

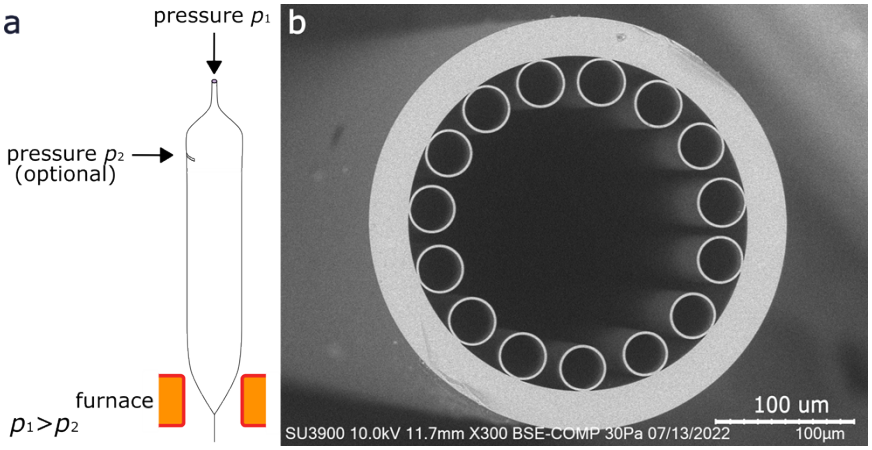

Fig. 7. (a) Drawing the stack to fiber whilst applying a positive pressure to the resonators through the working end. The core can also be pressurized through the slit to maintain a constant pressure differential between the cladding and the core. (b) An optical micrograph of a 15-resonator, multimode nodeless ARF with an outer diameter of 300 µm that we drew directly from stack to fiber without using sealant.

3.2 Making canes with a similar structure to the intended fiber

The second example is to draw an SSED stack to cane instead of fiber under positive pressure (as described in section 3.1). Two-stage drawing via a cane is necessary for smaller fibers guiding shorter-wavelength light while controlling the microstructure [23]. (The fiber of the previous section guided mid-IR light.) Since the deformation under surface tension of an ARF's microstructure as it is drawn is an inherently unstable process, it can be helpful to minimize the necessary deformation by making the cane as similar as possible to the desired fiber. This requires the application of pressure to the stack as it is drawn to cane, which is enabled by SSED. The ability to pressurize a cane gives an extra element of control over the two-stage fabrication process.

The example in Fig. 8 was part of a study of novel fiber designs. The stack had 12 resonator tubes that were allowed to expand by the application of positive pressure as the stack was drawn to cane. This is like the 'ice-cream cone' structure with an increased number of cladding elements [26,27]. Drawing the canes under pressure using SSED allowed us to control their

internal structure to replicate that of the intended fiber, but on a larger scale. Hence, the cross-sectional structure of the cane in Fig. 8(b) and the fiber in Fig. 8(c) are very similar.

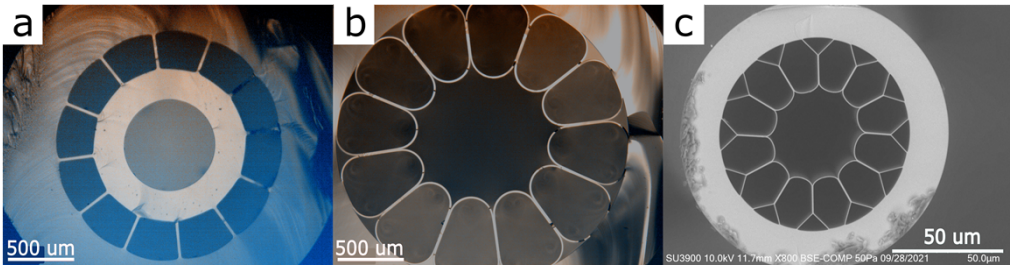

Fig. 8. (a) A cross-sectional optical micrograph of an SSED stack's working end, designed so that it could be drawn to canes under positive pressure. The cladding has twelve touching elements, so the stack includes twelve resonators and one sealed central support. (b) A cross-sectional optical micrograph of a cane drawn under positive pressure from the stack. (c) An SEM image of ARF drawn under pressure from the cane.

3.3 Microstructured resonators

The final example is the drawing of microstructured resonators from an SSED stack. Whereas in the previous examples the resonators were simple tubes, here we first need to draw individual compound resonators as canes from a stack. These resonator canes are then used instead of simple tubes as elements within another stack. For this example (again part of a study of novel fiber designs) the resonators have an inner and an outer tube, both of antiresonant thickness. However, unlike a nested structure where inner and outer tubes contact each other directly and so are not concentric, here we hold the inner tube centrally inside the outer tube using thin silica struts.

Fig. 9. (a) An optical micrograph of a microstructured resonator drawn using SSED. (b) A photograph of a stack incorporating the microstructured resonators, ready to be drawn into canes using another SSED step. The stack has a 25 mm outer diameter. (c) An optical micrograph of an ARF with microstructured resonators.

To make the microstructured resonators, we applied the SSED method on a stack comprising a ring of 8 smaller tubes packed snugly between a larger central tube and the outer jacket. The stack was drawn to resonator canes, Fig. 9(a), while completely closing the interstitial air region under negative pressure. Next, we assembled a new stack from the resonator canes and support tubes, Fig. 9(b), applied the SSED method to it, drew the stack into cane under positive pressure, and in turn drew the cane to fiber, Fig. 9(c).

We recognize that the nodes in this structure are likely to be detrimental to optical performance. However, we included this example to show that SSED allows non-circular structures to be fabricated more easily than would be possible using conventional techniques because it enables a stack to be drawn under pressure without the use of any sealants. SSED therefore opens new possibilities in the fabrication of antiresonant fibers with microstructured resonators; we are no longer limited to resonators with a circular cross-section, nor to nested structures.

4. Conclusions

We have described the SSED fabrication method that allows an ARF stack to be selectively pressurized without using a sealant to isolate hollow regions of the stack from one another. Instead, controlled fusion of glass elements at either end of the stack performs this purpose. Using examples of fibers that we have fabricated using SSED, we demonstrated three advantages that our method has over the unimproved two-stage stack and draw technique. SSED can be used to draw directly from stack to ARF without a cane stage, allowing significantly longer lengths of fiber to be collected than possible from a cane. SSED can also be used to draw canes under pressure such that they are structurally similar to the fiber they will be used to create. Finally, SSED can be used to create new types of microstructured resonators that would be impossible to fabricate without a means to draw a stack under positive and negative pressure.

Funding. Work was supported by UKRI grants EP/S001123/1 and EP/R005257/1.

Acknowledgments. We would like to thank Kristina R. Rusimova and Jonathan C. Knight for their comments on a draft of the manuscript.

Disclosures. The authors declare no conflicts of interest.

Data availability. Data underlying the results presented in this paper are in Ref. [28].

References

1. J. D. Shephard, A. Urich, R. M. Carter, P. Jaworski, R. R. J. Maier, W. Belardi, F. Yu, W. J. Wadsworth, J. C. Knight and D. P. Hand "Silica hollow core microstructured fibers for beam delivery in industrial and medical applications," Frontiers Phys. **3**, 24 (2015).
2. Marco Andreana, Tuan Le, Wolfgang Drexler, and Angelika Unterhuber, "Ultrashort pulse Kagome hollow-core photonic crystal fiber delivery for nonlinear optical imaging," Opt. Lett. **44**, 1588-1591 (2019).
3. J. D. Shephard, W. N. MacPherson, R. R. J. Maier, J. D. C. Jones, D. P. Hand, M. Mohebbi, A. K. George, P. J. Roberts, and J. C. Knight, "Single-mode mid-IR guidance in a hollow-core photonic crystal fiber," Opt. Express **13**, 7139-7144 (2005).
4. F. Yu, W. J. Wadsworth, and J. C. Knight, "Low loss silica hollow core fibers for 3–4 μm spectral region," Opt. Express **20**, 11153-11158 (2012).
5. F. Gebert, M. H. Frosz, T. Weiss, Y. Wan, A. Ermolov, N. Y. Joly, P. O. Schmidt, and P. St. J. Russell, "Damage-free single-mode transmission of deep-UV light in hollow-core PCF," Opt. Express **22**, 15388-15396 (2014).
6. F. Yu, M. Cann, A. Brunton, W. Wadsworth, and J. Knight, "Single-mode solarization-free hollow-core fiber for ultraviolet pulse delivery," Opt. Express **26**(8), 10879–10887 (2018).
7. SF. Gao, YY. Wang, W. Ding, and P. Wang, "Hollow-core negative-curvature fiber for UV guidance," Opt. Lett. **43**, 1347-1350 (2018).
8. R. Yu, Y. Chen, L. Shui, and L. Xiao "Hollow-Core Photonic Crystal Fiber Gas Sensing," Sensors. **20**(10), 2996 (2020).
9. N. V. Wheeler, M. N. Petrovich, R. Slavík, N. Baddela, E. Numkam, J. R. Hayes, D. R. Gray, F. Poletti, and D. J. Richardson, "Wide-bandwidth, low-loss, 19-cell hollow core photonic band gap fiber and its potential for low latency data transmission," in *National Fiber Optic Engineers Conference*, OSA Technical Digest (Optica Publishing Group, 2012), paper PDP5A.2.
10. B. Zhu, B. J. Mangan, T. Kremp, G. S. Puc, V. Mikhailov, K. Dube, Y. Dulashko, M. Cortes, Y. lian, K. Marceau, B. Violette, D. Cartsounis, R. Lago, B. Savran, D. Inniss, and D. J. DiGiovanni, "First Demonstration of Hollow-Core-Fiber Cable for Low Latency Data Transmission," in *Optical Fiber Communication Conference Postdeadline Papers 2020*, (Optica Publishing Group, 2020), paper Th4B.3.
11. N. M. Litchinitser, A. K. Abeeluck, C. Headley, and B. J. Eggleton, "Antiresonant reflecting photonic crystal optical waveguides," Opt. Lett. **27**, 1592-1594 (2002).
12. F. Poletti, "Nested antiresonant nodeless hollow core fiber," Opt. Express **22**, 23807-23828 (2014).
13. B. Debord, A. Amsanpally, M. Chafer, A. Baz, M. Maurel, J. M. Blondy, E. Hugonnot, F. Scol, L. Vincetti, F. Gérôme, and F. Benabid, "Ultralow transmission loss in inhibited-coupling guiding hollow fibers," Optica **4**, 209-217 (2017).
14. SF. Gao, YY. Wang, W. Ding, DL. Jiang, S. Gu, X. Zhang, and P. Wang, "Hollow-core conjoined-tube negative-curvature fibre with ultralow loss," Nat Commun **9**(1), 2828 (2018).
15. T. D. Bradley, J. R. Hayes, Y. Chen, G. T. Jasion, S. R. Sandoghchi, R. Slavik, E. N. Fokoua, S. Bawn, H. Sakr, I.A. Davidson, A. Taranta, J. P. Thomas, M. N. Petrovich, D.J. Richardson, and F. Poletti, "Record Low-Loss 1.3dB/km Data Transmitting Antiresonant Hollow Core Fibre," in *2018 European Conference on Optical Communication (ECOC)*, 1-3 (2018).

16. G. T. Jasion, T. D. Bradley, K. Harrington, H. Sakr, Y. Chen, E. N. Fokoua, I. A. Davidson, A. Taranta, J. R. Hayes, D. J. Richardson, and F. Poletti, "Hollow Core NANF with 0.28 dB/km Attenuation in the C and L Bands," in *Optical Fiber Communication Conference Postdeadline Papers 2020*, (Optica Publishing Group, 2020), paper Th4B.4.
17. H. Sakr, T. D. Bradley, G. T. Jasion, E. N. Fokoua, S. R. Sandoghchi, I. A. Davidson, A. Taranta, G. Guerra, W. Shere, Y. Chen, J. R. Hayes, D. J. Richardson, and F. Poletti, "Hollow Core NANFs with Five Nested Tubes and Record Low Loss at 850, 1060, 1300 and 1625nm," in *Optical Fiber Communication Conference (OFC) 2021*, pp. 1-3.
18. G. T. Jasion, H. Sakr, J. R. Hayes, S. R. Sandoghchi, L. Hooper, E. N. Fokoua, A. Saljoghei, H. C. Mulvad, M. Alonso, A. Taranta, T. D. Bradley, I. A. Davidson, Y. Chen, D. J. Richardson, and F. Poletti, "0.174 dB/km Hollow Core Double Nested Antiresonant Nodeless Fiber (DNANF)," *2022 Optical Fiber Communications Conference and Exhibition (OFC)*, 1-3 (2022).
19. P. St.J. Russell, "Photonic Crystal Fibres," Science **299**(5605), 358-362 (2003).
20. G. T. Jasion, J. R. Hayes, N. V. Wheeler, Y. Chen, T. D. Bradley, D. J. Richardson, and F. Poletti, "Fabrication of tubular anti-resonant hollow core fibers: modelling, draw dynamics and process optimization," *Opt. Express* **27**, 20567-20582 (2019).
21. I. A. Bufetov, A. F. Kosolapov, A. D. Pryamikov, A. V. Gladyshev, A. N. Kolyadin, A. A. Krylov, Y. P. Yatsenko, and A. S. Biriukov, "Revolver hollow core optical fibers," Fibers. **6**(2), 39-64 (2018).
22. T. D. Bradley, G. T. Jasion, H. Sakr, I. A. Davidson, J. R. Hayes, A. Taranta, K. Harrington, E. N. Fokoua, Y. Chen, D. J. Richardson, and F. Poletti, "Towards low loss hollow core optical fibers," Proc. SPIE **11713**, 117130A (2021).
23. Y. Chen and T. A. Birks, "Predicting hole sizes after fibre drawing without knowing the viscosity," Opt. Mater. Express **3**, 346-356 (2013).
24. N. Wheeler, P. Shardlow, F. Poletti "Method for fabricating an optical fibre preform," WO/2019/008352 (10 January 2019).
25. B. Winter, T. A. Birks, and W. J. Wadsworth, "Multimode Hollow-Core Anti-Resonant Optical Fibres," in *Frontiers in Optics + Laser Science APS/DLS*, The Optical Society (Optica Publishing Group, 2019), paper JTu4A.18.
26. F. Yu, M. Xu, and J. C. Knight, "Experimental study of low-loss single-mode performance in anti-resonant hollow-core fibers," Opt. Express **24**, 12969-12975 (2016).
27. F. Yu, W. J. Wadsworth, and J. C. Knight, "Low loss silica hollow core fibers for 3–4 μm spectral region," *Opt. Exp*. **20**(10), 11153–11158 (2012).
28. L. Murphy, J. Stone, S. Yerolatsitis, T. Birks, 2022. *Dataset for "Stack, seal, evacuate, draw: A method for drawing hollow-core fiber stacks under positive and negative pressure".* Bath: University of Bath Research Data Archive. https://doi.org/10.15125/BATH-01170.